1   **Title: Root meristem growth factor 1 controls root meristem size through**

2   **reactive oxygen species signaling**

3   **Authors:** Masashi Yamada[1], Xinwei Han[1]†, Philip. N. Benfey[1]*

4   **Affiliations:**

5   [1] Department of Biology and HHMI, Duke University, Durham, NC 27710, USA.

6   *Correspondence to: philip.benfey@duke.edu

7   † Current address:

8   Constellation Pharmaceuticals, Cambridge, MA 02142, USA.

9   **Abstract:**

10   Stem cell niche and root meristem size are maintained by intercellular interactions and signaling

11   networks of a plant peptide hormone, Root Meristem Growth Factor 1 (RGF1). How RGF1

12   regulates root meristem development is an essential question to understand stem cell function.

13   Although five receptors of RGF1 have recently been identified, the downstream signaling

14   mechanism remains unknown. Here, we report a series of signaling events following RGF1

15   action. The RGF1-receptor pathway controls distribution of reactive oxygen species (ROS)

16   along the developmental zones of the *Arabidopsis* root. We identify a novel transcription factor,

17   *RGF1 INDUCIBLE TRANSCRIPTION FACTOR 1* (*RITF1*), which plays a central role in

18   mediating RGF1 signaling. Manipulating *RITF1* expression leads to redistribution of ROS along

19   the root developmental zones. Changes in ROS distribution, in turn, enhance the stability of the

20   PLETHORA2 (PLT2) protein, a master regulator of root stem cells. Taken together, our study

21   clearly depicts a signaling cascade initiated by RGF1 and links the RGF1 peptide to ROS

22   regulatory mechanisms.

23   **Text :**

24   Roots encounter various environmental conditions in soil and respond by altering their growth.

25   The *Arabidopsis* root has a simple cylindrical structure. Each layer of the cylinder consists of a

26   different cell-type, which is generated from a stem cell population at the root tip, and develops

27   into mature cells along the longitudinal axis of the root. Developmental stages are defined as the

28   meristematic zone, the elongation zone, and the differentiation zone. Root growth arises through

29   controlled cell division in the meristematic zone and subsequent cell elongation and

30   differentiation in the elongation and differentiation zones. During the transition to differentiation,

31   most cells arrest division and increase their size through post-mitotic cell expansion. The size of

32   the developmental zones is determined by intrinsic and extrinsic signals. In the *Arabidopsis* root,

33   superoxide (O_2^-) and hydrogen peroxide (H_2O_2) exhibit distinct distribution patterns along the

34   developmental zones[1]. Superoxide primarily accumulates in dividing cells in the meristematic

35   zone, while hydrogen peroxide mainly accumulates in elongated cells in the differentiation

36   zone[1,2]. The balance between O_2^- and H_2O_2 modulates the transition from proliferation to

37   differentiation[2]. The *UPBEAT1* (*UPB1*) gene regulates meristematic zone size by restricting

38   H_2O_2 distribution in the elongation zone[2]. These findings have demonstrated that reactive oxygen

39   species (ROS) are an intrinsic signal involved in establishing the size of the meristematic zone.

40   The RGF1 peptide is also able to control the size of the meristematic zone both as an

41   intrinsic signal and when extrinsically applied [3-5]. External treatment with RGF1 increases the

42   size of the meristematic zone, while the *rgf1/2/3* triple mutant has a smaller meristematic zone[3].

43   Five receptor-like kinases have been identified as RGF1 receptors [6-8]. Quintuple mutants of

44   these receptors lack most of the cells in the root meristem and are insensitive to RGF1,

45   demonstrating that the RGF signaling pathway controls root meristem size via these receptors[8].

46   The RGF1 signaling pathway controls the stability of the PLETHORA (PLT) 1/2 proteins[3],

2

47   which are required for stem cell maintenance[9]. However, it is not known how RGF modulates

48   the size of the meristematic zone and the stability of the PLT1/2 proteins. Here, we show that the

49   RGF1 signaling pathway modulates ROS distribution along the three root developmental zones

50   effectively controlling the size of the meristematic zone. Changes in ROS distribution result in

51   changes in stability of the PLT2 protein. Transcriptome analysis after RGF1 treatment identified

52   elevated expression of a meristematic zone-specific novel transcription factor (*RITF1*). Over-

53   expression of the *RITF1* gene phenocopies the enlarged meristematic zone and altered

54   distribution of ROS signaling upon RGF1 treatment.

55   It has been reported that RGF1 modulates meristematic zone size[3,6-8]. To confirm the effect of

56   RGF1 treatment on the meristematic zone with greater specificity, we used the meristematic

57   zone-specific marker HIGH PLOIDY2 (HPY2)-GFP protein[10] (Fig. 1a and b). HPY2-GFP was

58   detected in an enlarged area 24h after RGF1 treatment (Fig. 1a-e) and this correlated with a

59   larger meristematic zone (Fig. 1c and d). These results combined with defects in the meristematic

60   zone in *rgf* and *rgf1 receptor* (*rgfr*) mutants suggest that RGF1 controls gene expression

61   primarily in the meristematic zone. Therefore, we performed a meristematic zone-specific

62   transcriptome analysis to uncover the molecular mechanism underlying the RGF1 signaling

63   pathway. To identify primary target genes upon RGF1 treatment, we isolated the meristematic

64   zone based on the *HPY2-GFP* signal one hour after RGF1 treatment (Fig. 1f).

65   Since the expression of *HPY2-GFP* and the size of the meristematic zone were unchanged in this

66   time period (data not shown), we can exclude the possibility that an enlarged meristem is the

67   reason for elevated RNA levels. Expression of 583 genes was significantly altered in the RNA-

68   seq data between RGF1 and mock treatment (FDR-adjusted p value < 0.1) (Extended Data).

69   Most differentially expressed genes were positively regulated by RGF1 treatment. However, our

3

70   transcriptome analysis revealed specific down-regulation of *RGF1* itself, suggesting negative

71   feed-back regulation (Extended Data). Significantly enriched Gene Ontology (GO) categories

72   included "oxidoreductase activity" (p= 4.90E-06) and "oxidation reduction" (p= 4.90E-05)

73   (Extended Data Fig. 1 and Extended Data). These data suggested that RGF1 might signal

74   through a ROS intermediate to control the size of the meristematic zone.

75   To examine the relationship between RGF1 and ROS signaling, we analyzed the distribution

76   of superoxide and hydrogen peroxide after RGF1 treatment. The specific indicator H_2O_2-3'-O-

77   Acetyl-6'-O-pentafluorobenzenesulfonyl-2'-7'-difluorofluorescein-Ac $(H_2O_2$-BES-Ac$)^2$ for

78   hydrogen peroxide exhibited lower fluorescence in the meristematic and elongation zones 24 h

79   after RGF1 treatment (Fig. 2a and c). Superoxide signals were detected by nitroblue tetrazolium

80   (NBT) staining[1] and observed more broadly in the meristematic and elongation zone 24 h after

81   RGF1 treatment (Fig. 2b and d). To determine if these changes in ROS distributions depend on

82   the RGF1 receptors, ROS signals were detected in the *rgfr1/2/3* triple mutant. The *rgfr1/2/3*

83   triple mutant was insensitive to RGF1 and did not form a larger meristematic zone upon RGF1

84   treatment (Fig.2e). Levels of H_2O_2 and O_2^- in the *rgfr1/2/3* triple mutant were comparable

85   between mock and RGF1 treatments (Fig. 2e-h). These data are consistent with our hypothesis

86   that the RGF1-receptor signaling pathway controls the size of the meristematic zone via ROS.

87   It was previously reported that the RGF1 signaling pathway regulates PLT1/2 post-

88   translationally[6]. We compared signals from a *PLT2* transcriptional fusion line; *promoter PLT2*

89   *(pPLT2)-CFP[11]* and from a *PLT2* translational fusion line; *genomic PLT2 (gPLT2)-YFP[11]*

90   (Extended Data Fig. 2a-c) and observed broader localization of *gPLT2-YFP* signals 24 h after

91   RGF1 treatment (Extended Data Fig. 2b-d). However, the levels and localization of *pPLT2-CFP*

92   were comparable between Mock and RGF1 treatments (Extended Data Fig. 2a), even though

4

93   RGF1-treated roots had a larger meristematic zone. These experiments confirmed that RGF1

94   regulates PLT2 post-translationally. We detected the highest levels of *gPLT2-YFP* and *pPLT2-*

95   *CFP* in the cells around the QC (Extended Data Fig. 2a and b). The *gPLT2-YFP* signal gradually

96   declined in the meristem after mock treatment (Extended Data Fig. 2b). However, after RGF1

97   treatment, the *gPLT2-YFP* signal decreased more gradually and was broadly localized in a larger

98   meristematic zone (Extended Data Fig. 2c). Since proteasome-dependent degradation of proteins

99   occurs in the presence of elevated H_2O_2 levels[12,13], we hypothesized that broader localization of

100   the PLT2 protein is due to the decreased H_2O_2 and increased O_2^- levels upon RGF1 treatment as

101   shown in Figure 2. To determine if H_2O_2 can decrease the stability of the PLT2 protein, we

102   treated the *gPLT2-YFP* line with RGF1 and H_2O_2. H_2O_2 treatment inhibited the size increase of

103   the meristem upon RGF1 treatment (Extended Data Fig. 3d and e). Furthermore, *gPLT2-YFP*

104   signals were not localized as broadly in roots co-treated with RGF1 and H_2O_2 as compared with

105   roots only treated with RGF1 (Extended Data Fig. 3b and c). These results are consistent with

106   our hypothesis that lower H_2O_2 levels enhance the stability of the PLT2 protein. To further probe

107   the relationship between PLT2 protein stability and ROS, we measured *gPLT2-YFP*, O_2^-, and

108   H_2O_2 in a shorter time course (4-10h) after RGF1 treatment. At 6 h after RGF1 treatment, we

109   began to detect broader localization of *gPLT2-YFP* (Fig. 3a and b, Extended Data Fig. 4). At the

110   same time, increased superoxide levels, as indicated by broader staining with NBT, were

111   observed in the meristematic zone (Fig. 3g and h) along with lower signals of H_2O_2-BES-Ac in

112   the distal side of the meristematic zone (Fig. 3m and n, white arrows). At 8 h and 10 h after

113   RGF1 treatment, expanded *gPLT2-YFP* expression and O_2^- signals correlated with declining

114   H_2O_2 signals (Fig. 3c-f, 3i-l, 3o-r and Extended Data Fig. 4a-c). These data indicate that RGF1

115   treatment increases root meristem size and PLT2 protein stability by modulating ROS levels.

5

116   To identify for downstream factors that mediate the RGF1/ROS signaling pathway, we

117   combined our RGF1 treatment transcriptome data with our previously published transcriptome

118   data from the three root developmental zones[14]. We looked for genes whose expression was

119   induced by RGF1 and specific to the meristematic zone. The *PLANT AT-RICH SEQUENCE and*

120   *ZINC-BINDING TRANSCRIPTION FACTOR* (*PLATZ*) *FAMILY PROTEIN* gene (AT2G12646)

121   is strongly expressed in the meristematic zone with lower expression in the elongation zone and

122   greatly reduced expression in the differentiation zone (Extended Data Fig. 5a). As this gene has

123   not been characterized, we named it *RGF1 INDUCIBLE TRANSCRIPTION FACTOR* 1 (*RITF1*).

124   Expression of *RITF1* increased approximately 2-fold after 1 h of RGF1 treatment (Extended

125   Data and Extended Data Fig. 5b). To understand its function, *RITF1*was inducibly over-

126   expressed using the estradiol inducible promoter system[15]. After 24 h of 10μM β-estradiol

127   treatment, the meristematic zone became enlarged and the number of cells increased as compared

128   with mock treatment (Fig. 4a and b). These phenotypes are very similar to RGF1 treated roots.

129   Changes in ROS levels could also be detected in the *RITF1* over-expression line (Fig. 4c-4f).

130   H_2O_2 levels declined in all three developmental zones upon estradiol treatment (Fig. 4c and 4d).

131   Furthermore, ectopic over-expression of *RITF1* enhanced O_2^- signals in a broader area in the

132   meristematic zone (Fig. 4e) and ectopic O_2^- signals were detected in the elongation and

133   differentiation zone (Fig. 4e, a blue arrow and 4f), where RGF1 receptors are not expressed[6].

134   This suggests that the *RITF1* gene may control ROS levels without other downstream regulators

135   of the RGF1 signaling pathway.

136   The larger meristematic zone and alteration of ROS signals by over-expression of *RITF1*

137   strongly suggest that the *RITF1* gene is a primary regulator controlling ROS signaling and

138   meristem size in the RGF1 signaling pathway. Furthermore, the *ritf1* mutant (T-DNA insertion

6

139   line) has a root growth defect with a smaller meristematic zone (Extended Data Fig. 5c and 5d),

140   and exhibits resistance to RGF1 (Extended Data Fig. 5d and 5e). Taken together, these results

141   indicate that RGF1 modulates ROS levels and root meristem size by controlling expression of

142   the *RITF1* gene.

143   We have previously reported that UPB1 reduces H_2O_2 levels and controls meristem size by

144   down-regulating peroxidase genes in the elongation zone[2]. Our transcriptome analysis didn't find

145   significant changes in *UPB1* expression upon RGF1 treatment (Extended Data). We did find

146   elevated expression of 5 peroxidase genes (Extended Data), but these are not downstream targets

147   of *UPB1*[2], suggesting that RGF1 regulates meristem size independently of *UPB1*. However, it is

148   still possible that RGF1 controls meristem size via these peroxidases. To determine if the

149   peroxidase genes upregulated by RGF1 play a role in meristem size control in the RGF1

150   signaling pathway, we over-expressed two of them (At5g39580 and At4g08780). In neither case

151   did we observe a larger meristematic zone (data not shown).

152   Identification of the RGF1 peptide and its receptors has provided a novel pathway for

153   regulation of root growth [3-8]. Initially, it was shown that this signaling pathway regulates root

154   meristem size by enhancing PLT1/2 stability [3,6,8]. However, the underlying mechanism was not

155   elucidated. We show that RGF1 can modulate ROS levels in the meristematic zone over

156   relatively short time periods and that longer RGF1 treatment results in altered distributions of

157   ROS along the developmental zones of the root. Moreover, PLT2 protein localization correlates

158   with ROS distribution and elevated H_2O_2 levels reduce the stability of the PLT2 protein even in

159   the presence of RGF. Finally, we identified a novel transcription factor, *RITF1*, that is induced

160   by RGF1 in the meristematic zone and can alter ROS levels and meristem size. Taken together,

161   our results show that the RGF1 signaling pathway modulates ROS levels and distribution by up-

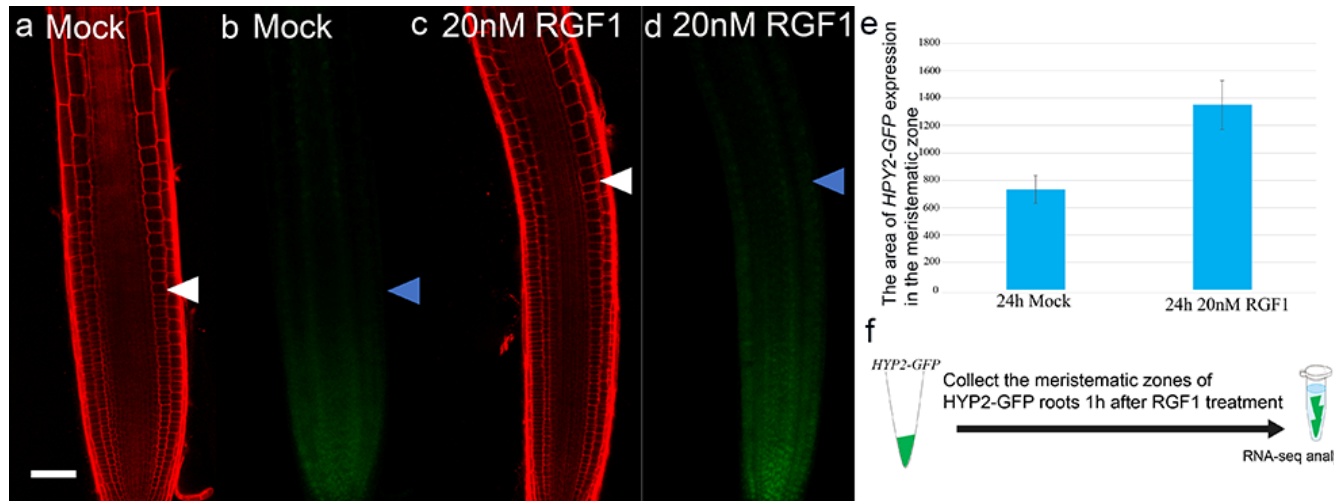162   regulating the *RITF1* gene in the meristematic zone.

163   **Figures:**

164
165   **Figure 1. Expression of meristematic zone marker and transcriptome analysis upon RGF1**

166   **treatment.** Confocal images of *HPY2-GFP* are shown 24 h after treatments with water (mock) (a

167   and b) and 20 nM RGF1 (c and d). Seedlings were grown on MS medium for seven days before

168   treatment. Propidium iodide stained roots (a and c); GFP signals (b and d). White and blue arrow

169   heads indicate the junction between the meristematic zone and the elongation zone. Scale bar =

170   50 µm (e) Area (µm^2) of *HPY2-GFP* expression is shown. Error bars represent ± standard

171   deviation (SD; n≥9). (f) Schematic of RNA extraction following RGF1 treatment.

172
173
174
175
176
177
178
179

8
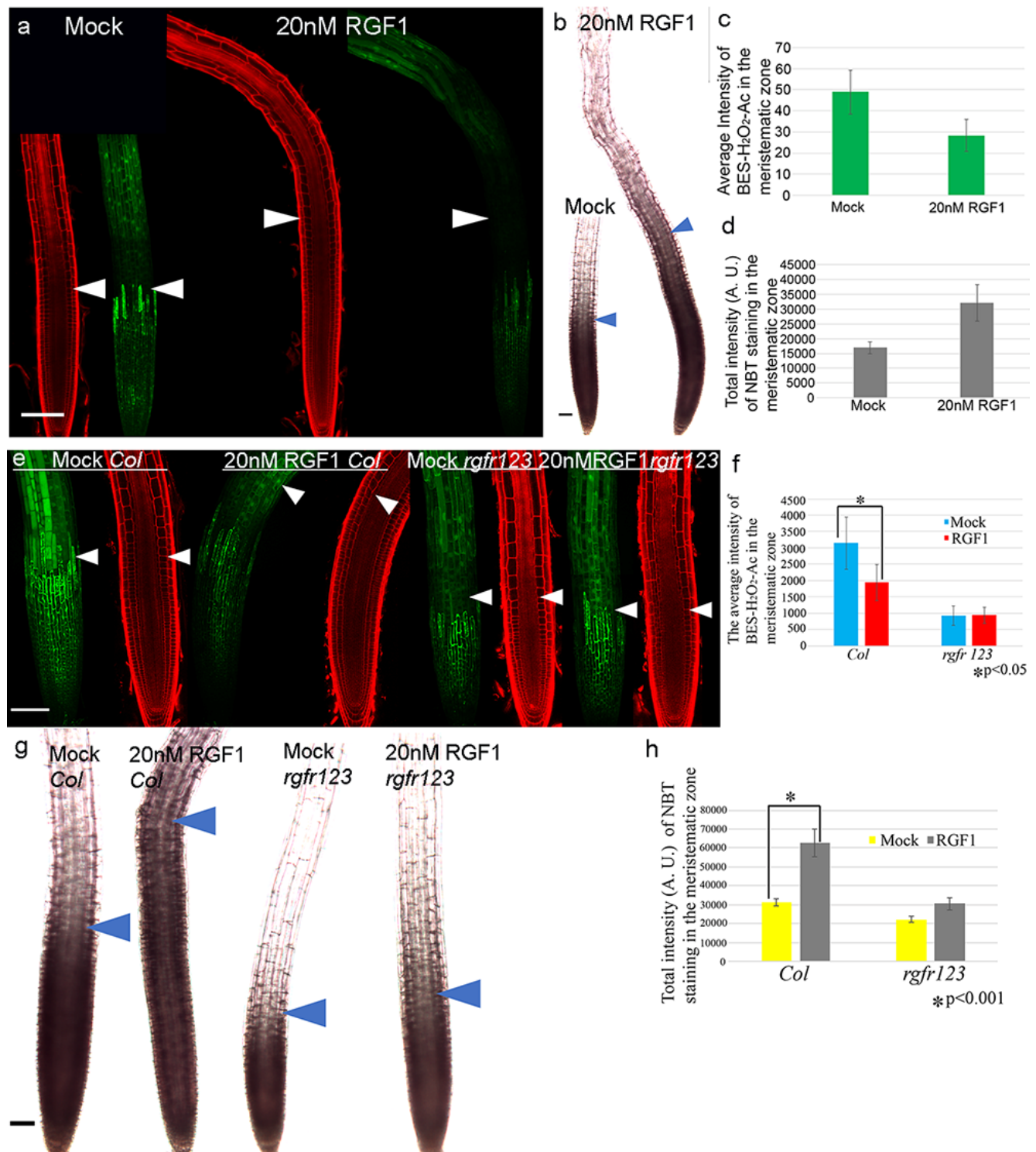
180

181 **Figure 2. Distribution of ROS levels upon RGF1 treatment.** (a). Confocal images of roots 24

182 h after treatment with Water (mock) and 20 nM RGF1 (right). Propidium iodide (PI) staining

183   (red images), H_2O_2-BES-Ac fluorescence (green images). (b) Roots stained with NBT 24 h after

184   treatment with mock or 20 nM RGF1 (right). (c) Quantification of H_2O_2-BES-Ac intensity in

185   meristematic zone (n = 6, ± SD; p < 0.003). (d) Quantification of NBT staining intensity

186   (arbitrary units (A.U.) values) in meristematic zone (n≥8, ± SD; p < 0.001). (e) Confocal images

187   of roots 24 h after treatment with mock or 20 nM RGF1 in wild type (Col-0) (left four images) or

188   the *rgfr 1/2/3* triple mutant (right four images). PI staining (red images). H_2O_2-BES-Ac

189   fluorescence (green images). (f) Quantification of H_2O_2-BES-Ac staining intensity in the

190   meristematic zone in wild type and the *rgfr 1/2/3* triple mutant (n = 5, ± SD; *p < 0.05). (g)

191   Roots stained with NBT 24 h after treatment with mock or 20 nM RGF1 in wild type (left two

192   images) or the *rgfr 1/2/3* mutant (right two images). (h) Quantification of NBT staining intensity

193   (A.U. values) in the meristematic zone in wild type or the *rgfr 1/2/3* triple mutant (n = 5, ± SD;

194   *p < 0.001). White and blue arrowheads indicate the junction between the meristematic zone and

195   elongation zone. Scale bar = 50 µm. Seedlings were grown on MS medium for seven days before

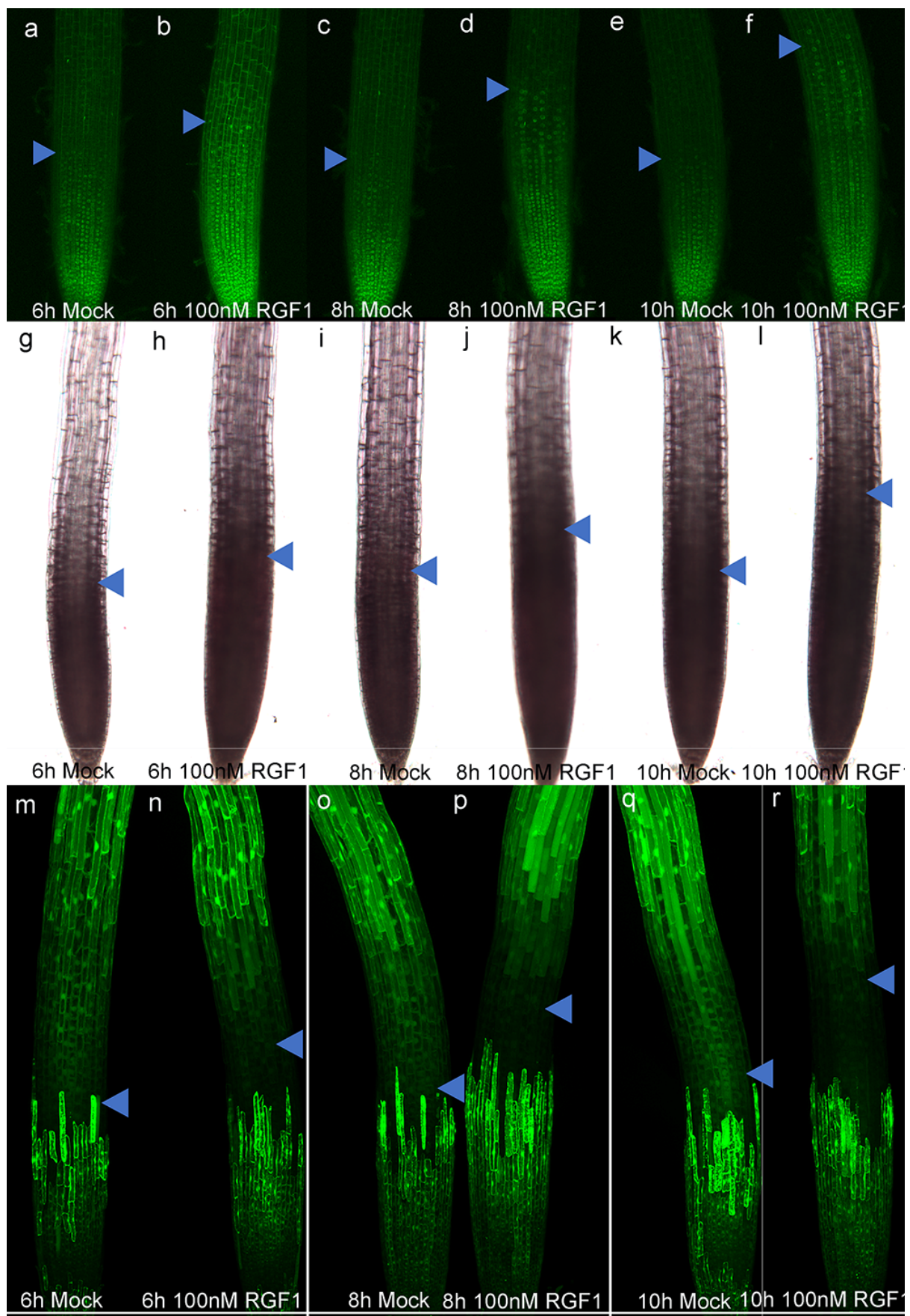196   treatment.

197

198

199

200

201

202

203

204

205

206

207

208

209

210

11

211 **Figure 3. Localization of gPLT2-YFP, NBT, and H$_2$O$_2$-BES-Ac after RGF1 treatment.**

212 Localization of gPLT2-YFP, NBT, (M-R) H$_2$O$_2$-BES-Ac, 6 h after treatment with water (mock)

213 (a, g, and m) or 100 nM RGF1 (b, h, and n), 8 h after treatment with mock (c, i, and o), or 100

214 nM RGF1 (d, j, and p). 10h after treatment with mock (e, k, and q) or 100nM RGF1 (f, l, and r).

215 Blue arrow heads indicate junction between meristematic zone and elongation zone. Scale bar =

216 50 µm. Seedlings were grown on MS agar plates for seven days before treatment.

217

218

219

220

221

222

223

224

225

226

227

228

229

230

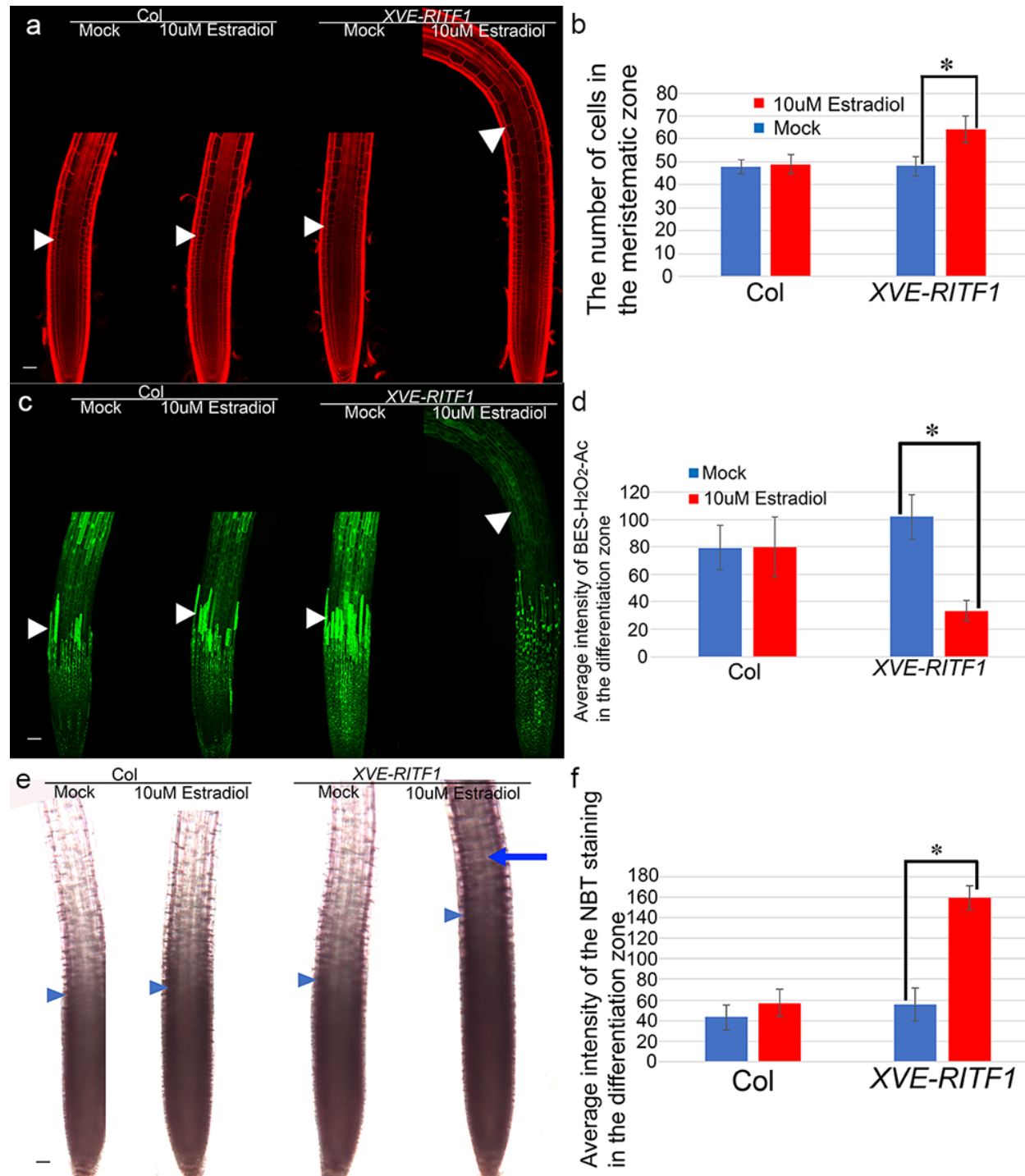231

232

233

234

235

236

237

238

239

240

241

Figure 4. Over-expression of *RITF1*.(a) Confocal images (left WT, right *XVE-RITF1*) of PI stained roots. (b) Number of cells in meristematic zone in wild type (Col) and *XVE-RITF1* 24h after mock or 10μM Estradiol treatment. (N=6, ±SD, and *p<0.001). (c) Confocal images (left

13

245   WT, right *XVE-RITF1*) of H_2O_2-BES-Ac stained roots. (d) Average intensity of BES-H_2O_2-Ac in

246   differentiation zone 24h after mock or 10μM Estradiol treatments. (N=6, ±SD, and *p<0.001).

247   (e) Light microscope images of NBT stained roots. Seedlings were grown on MS agar plates for

248   seven days before mock or 10μM estradiol treatment. (f) Average intensity of NBT staining in

249   differentiation zone 24h after mock or 10μM Estradiol treatments. (N≥7, ±SD, and *p<0.001).

250   Scale bar=50μm. White and blue arrow heads show the junction between the meristematic zone

251   and the elongation zone.

252   **Methods:**

253   **Plant materials and growth conditions**

254   All *Arabidopsis* mutants and marker lines used in this research are in the Columbia-0 (Col-0)

255   background. The T-DNA insertion line *ritf1* (SALK_081503C) was obtained from the

256   Arabidopsis Biological Resource Center at Ohio State University. The T-DNA insertion was

257   identified at 787 bp downstream of the transcription start site in the ritf1 mutant. Seeds were

258   surface sterilized using 50% (vol/vol) bleach and 0.1% Tween20 (Sigma) for 15 min and then

259   rinsed five times with sterile water. All seeds were plated on standard MS media (1× Murashige

260   and Skoog salt mixture, Caisson Laboratories), 0.5 g/L MES, 1% Sucrose, and 1% Agar (Difco)

261   and adjusted to pH 5.7 with KOH. All plated seeds were stratified at 4°C for 2 d before

262   germination. Seedlings were grown on vertically positioned square plates in a Percival incubator

263   with 16 h of daily illumination at 22 °C.

264

265   **Detecting *gPLT2-YFP* and ROS signals**

266   The seedlings of wild type and the *rgfr1/2/3* mutant were grown for six days on MS agar plates,

267   then transferred to MS agar plates containing either water (mock) or 20 nM synthetic sulfated

268   RGF1 peptide (Invitrogen). After RGF1 treatment, seedlings were stained for 2 min in a solution

269   of 200μM NBT in 20mM phosphate buffer (pH 6.1) in the dark and rinsed twice with distilled

270   water. For hydrogen peroxide detection with BES-H_2O_2-Ac[16], seedlings were incubated in 50μM

271   of BES-H_2O_2-Ac (WAKO) for 30 min in the dark, then were mounted in 10 mg/mL propidium

272   iodide (PI) in water[2]. Roots were observed using a 20× objective lens under a Zeiss LSM 880

273   laser scanning confocal microscope. Excitation and detection windows were set as follows: BES-

274   H_2O_2-Ac, excitation at 488nm and detection at 500-550 nm; PI staining, excitation at 561 nm and

275   detection at 570-650 nm. Confocal images were processed, stitched, and analyzed using the Fiji

276   package of ImageJ[17]. The maximum projection image was produced from the z-section images of

277   BES-H_2O_2-Ac staining. The average intensity of BES-H_2O_2-Ac in the meristematic zone was

278   measured in 5 or 6 roots with three biological replicates. Images for NBT staining were obtained

279   using a 10x objective lens under a Leica DM5000-B light microscope. The total intensities of

280   NBT staining in the meristematic zone were measured in 10 roots with three biological replicates

281   using the Fiji software package[17].

282   For shorter time course experiments, seedlings of *gPLT2-YFP[11]* were grown on MS agar plates

283   for 6 days, then transferred to MS agar plates containing either water (mock) or 100nM RGF1

284   peptide. At 6, 8, and 10h after transfer to RGF1 plates, images were taken with a confocal or

285   light microscope after PI, NBT, and BES-H_2O_2-Ac staining, as previously described.

286

287   **Total RNA preparation, RNA amplification and library preparation for RNA-seq**

288   The *HYP2-GFP[10]* lines were grown on MS plates for 6 days. *HYP2-GFP* seedlings were then

289   transferred into liquid MS media and treated with water (mock) or 100nM RGF1 peptide in 6-

290   well-plates for 1h. After 1h treatment with mock or RGF1, the seedlings were taken out of liquid

15

291   MS media and transferred onto a 2% agarose plate. Using an ophthalmic scalpel (Feather), the

292   meristematic zone of the seedlings was precisely dissected based on *HYP2-GFP* fluorescence as

293   detected under a dissecting microscope (Axio Zoom, Zeiss). Total RNA was extracted from 20

294   root sections treated with mock or 100nM RGF1 using the RNeasy Micro Kit (Qiagen). For each

295   treatment, three replicates of the RNA extractions were performed. All total RNA samples were

296   treated with DNaseI during RNA extraction. RNA quality was examined using a 2100

297   Bioanalyzer (Agilent). The RNA Integrity Number (RIN) was over 9.0 in all samples. The

298   concentration of total RNA was measured by a Qubit (Invitrogen) instrument. For each replicate,

299   50ng total RNA was amplified using the Ovation RNA-seq System V2 (NuGEN). Following

300   amplification, 3μg of cDNA was fragmented using the Covaris S-Series System. 400ng of the

301   fragmented cDNA with an average size of 400bp was used for library preparation using the

302   Ovation Ultralow System V2 (NuGEN). Illumina sequencing was performed at the Duke

303   Genome Sequencing Shared Resource. The libraries for three biological replicates of mock and

304   RGF1 treated meristematic zones were sequenced on an Illumina HiSeq2000 (100 base-paired

305   reads).

306

307   **Differential expression analysis following RGF1 peptide treatment**

308   Illumina sequencing reads were mapped to TAIR10 Arabidopsis genome using Tophat V2.0.7.

309   The parameters used for mapping are as follows :"-N 5 --read-gap-length 5 --read-edit-dist 5 --

310   b2-sensitive -r 100 --mate-std-dev 150 -p 5 -i 5 -I 15000 --min-segment-intron 5 --max-segment-

311   intron 15000 --library-type fr-unstranded". To select properly mapped reads with unique

312   mapping positions, only alignments with flag of 83, 99, 147 or 163 and a mapping quality score

313   of 50 were kept for further analysis. Mapping positions of these reads were compared with the

16

314   Araport11 genome annotation

315   (https://www.araport.org/downloads/Araport11_Release_201606/annotation) using HTseq-count

316   generated read count per gene with parameters "--stranded=no --mode=intersection-nonempty".

317   The raw read counts of miRNA, lncRNA and protein coding genes were then used as input into

318   DESeq2 for differential gene expression analysis. Genes with an adjusted p-value less than or

319   equal to 0.1 were regarded as differentially expressed between RGF treatment and mock. The

320   enriched gene ontology groups among differentially expressed genes were identified as

321   Differences using agriGO (downloaded from http://geneontology.org). A customized GO

322   annotation was used that required a significance level of 0.01 and a minimum mapping entry of

323   10.

324

325   **Plasmid Construction**

326   The coding sequence of the *RITF1* gene (AT2G12646) was amplified using the Phusion High-

327   Fidelity DNA polymerase (New England Biolabs) from a wildtype cDNA library, and then sub-

328   cloned into the *pENTR/D/TOPO* vector (Invitrogen). The following primers were used for *RITF1*

329   amplification: 5'-CACCATGGGAATTCAGAAACCGG-3' and 5'-

330   TTAACAGAGAGGAGATCGTTG-3'. The sequence of the *RITF1* gene in *pENTR/D/TOPO*

331   vector was confirmed by Sanger sequencing. The clone was recombined with the *pMDC7*

332   vector[15] using LR clonase II (Invitrogen) to fuse the estradiol inducible promoter (XVE)[18] and

333   the coding region of the *RITF1* gene.

334

335   **Measurement of meristem size and detection of ROS signals after over-expression of the**

336   ***RITF1* gene**

17

337   The ***XVE-RITF1*** construct was transformed into wild type (Col). To measure meristem size and

338   detect ROS signals, two independent lines of *XVE-RITF1* and wild-type were grown on MS

339   media for six days, then transferred to MS media containing DMSO (Mock) and 10μM β-

340   estradiol (Sigma). After 24h treatment with mock or estradiol, meristem size and ROS signals

341   were measured and detected in wild type and the *XVE-RITF1* lines, as described in the previous

342   section.

343

344   **References:**

345   1   Dunand, C., Crevecoeur, M. & Penel, C. Distribution of superoxide and hydrogen

346   peroxide in Arabidopsis root and their influence on root development: possible

347   interaction with peroxidases. *New Phytol* **174**, 332-341, doi:10.1111/j.1469-

348   8137.2007.01995.x (2007).

349   2   Tsukagoshi, H., Busch, W. & Benfey, P. N. Transcriptional regulation of ROS controls

350   transition from proliferation to differentiation in the root. *Cell* **143**, 606-616,

351   doi:10.1016/j.cell.2010.10.020 (2010).

352   3   Matsuzaki, Y., Ogawa-Ohnishi, M., Mori, A. & Matsubayashi, Y. Secreted peptide

353   signals required for maintenance of root stem cell niche in Arabidopsis. *Science* **329**,

354   1065-1067, doi:10.1126/science.1191132 (2010).

355   4   Whitford, R. *et al.* GOLVEN secretory peptides regulate auxin carrier turnover during

356   plant gravitropic responses. *Dev Cell* **22**, 678-685, doi:10.1016/j.devcel.2012.02.002

357   (2012).

358   5   Meng, L., Buchanan, B. B., Feldman, L. J. & Luan, S. CLE-like (CLEL) peptides control

359   the pattern of root growth and lateral root development in Arabidopsis. *Proc Natl Acad*

360   *Sci U S A* **109**, 1760-1765, doi:10.1073/pnas.1119864109 (2012).

361   6   Shinohara, H., Mori, A., Yasue, N., Sumida, K. & Matsubayashi, Y. Identification of

362   three LRR-RKs involved in perception of root meristem growth factor in Arabidopsis.

363   *Proc Natl Acad Sci U S A* **113**, 3897-3902, doi:10.1073/pnas.1522639113 (2016).

364   7   Song, W. *et al.* Signature motif-guided identification of receptors for peptide hormones

365   essential for root meristem growth. *Cell Res* **26**, 674-685, doi:10.1038/cr.2016.62 (2016).

366   8   Ou, Y. *et al.* RGF1 INSENSITIVE 1 to 5, a group of LRR receptor-like kinases, are

367   essential for the perception of root meristem growth factor 1 in Arabidopsis thaliana. *Cell*

368   *Res* **26**, 686-698, doi:10.1038/cr.2016.63 (2016).

369   9   Aida, M. *et al.* The PLETHORA genes mediate patterning of the Arabidopsis root stem

370   cell niche. *Cell* **119**, 109-120, doi:10.1016/j.cell.2004.09.018 (2004).

371   10   Ishida, T. *et al.* SUMO E3 ligase HIGH PLOIDY2 regulates endocycle onset and

372   meristem maintenance in Arabidopsis. *Plant Cell* **21**, 2284-2297,

373   doi:10.1105/tpc.109.068072 (2009).

374   11   Galinha, C. *et al.* PLETHORA proteins as dose-dependent master regulators of

375   Arabidopsis root development. *Nature* **449**, 1053-1057, doi:10.1038/nature06206 (2007).

376   12   Kurepa, J. & Smalle, J. A. To misfold or to lose structure?: Detection and degradation of

377   oxidized proteins by the 20S proteasome. *Plant Signal Behav* **3**, 386-388 (2008).

378   13   Shringarpure, R., Grune, T., Mehlhase, J. & Davies, K. J. Ubiquitin conjugation is not

379   required for the degradation of oxidized proteins by proteasome. *J Biol Chem* **278**, 311-

380   318, doi:10.1074/jbc.M206279200 (2003).

381   14   Li, S., Yamada, M., Han, X., Ohler, U. & Benfey, P. N. High-Resolution Expression Map

382   of the Arabidopsis Root Reveals Alternative Splicing and lincRNA Regulation. *Dev Cell*

383   **39**, 508-522, doi:10.1016/j.devcel.2016.10.012 (2016).

384   15   Curtis, M. D. & Grossniklaus, U. A gateway cloning vector set for high-throughput

385   functional analysis of genes in planta. *Plant Physiol* **133**, 462-469,

386   doi:10.1104/pp.103.027979 (2003).

387   16   Maeda, H. *et al.* Fluorescent probes for hydrogen peroxide based on a non-oxidative

388   mechanism. *Angew Chem Int Ed Engl* **43**, 2389-2391, doi:10.1002/anie.200452381

389   (2004).

390   17   Schindelin, J. *et al.* Fiji: an open-source platform for biological-image analysis. *Nat*

391   *Methods* **9**, 676-682, doi:10.1038/nmeth.2019 (2012).

392   18   Zuo, J., Niu, Q. W. & Chua, N. H. Technical advance: An estrogen receptor-based

393   transactivator XVE mediates highly inducible gene expression in transgenic plants. *Plant*

394   *J* **24**, 265-273 (2000).

395   **Supplementary Information** is available in the online version of the paper.

20

404   **Author contributions:**

405   M.Y. and P.N.B. conceptualized the study; M.Y. performed all experiments; X.H. performed

406   the computational analyses; all authors wrote the paper.

407   **Author information:**

408   Reprints and permissions information is available at www.nature.com/reprint. The authors

409   decleare competing financial interests: details are available in the online version of the paper.

410   Readers are welcome to comment on the online version of the paper. Correspondence and

411   requests for materials should be addressed to P.N.B. (philip.benfey@duke.edu).

412